sustainability

MDPI

Article

Probabilistic Seismic Hazard Analysis on Pavement Failure Restoration; Case Study of Sorong–Makbon Road

Lucky Caroles

Infrastructure Engineering Study Program, Graduate School of Hasanuddin University, Makassar 90242, Indonesia; luckycaroles@unhas.ac.id

Abstract: The Sorong–MakbonSorong–Makbon Corridor is one of the key routes connecting Sorong to other sections of the West Papua region in Indonesia. Throughout the Sorong–Makbon Corridor, roads and slopes often sustain damage. When landslides reach the road shoulder and destroy the pavement, they often prevent access to the road. In addition to the influence of surface water runoff, there are indications that earthquakes contribute to the ineffectiveness of the previous design. This seems to be accurate since the author has seen the typical movement of avalanches. Using the Probabilistic Seismic Hazard Analysis (PSHA) approach, the earthquake's effects on this corridor were mapped out. With the use of the Indonesian earthquake data library, the Matlab-Zmap Program, and the Spectrum Response, the history of earthquakes in the Sorong–Makbon corridor was analysed to determine their velocity. This analysis reveals that the earthquake's influence on the Sorong–Makbon corridor has an acceleration value between 1.2 and 1.5 G. The prior design did not account for a quake of this magnitude. With this study, the correctly identified seismic impact could be sent back into the simulation to more adequately repair and restore the damage.

Keywords: landslide; Papua; pavement; restoration; seismic; slope

check for updates

Citation: Caroles, L. Probabilistic Seismic Hazard Analysis on Pavement Failure Restoration; Case Study of Sorong–Makbon Road. *Sustainability* **2023**, *15*, 5994. https://doi.org/10.3390/su15075994

Academic Editor: Mohammad Mahdi Javidan

Received: 26 January 2023
Revised: 11 February 2023
Accepted: 17 February 2023
Published: 30 March 2023

1. Introduction

The increased risk of natural catastrophes is only a reflection of natural occurrences that are geographically specific to the Indonesian area. Indonesia is an archipelago where the Indo-Australian, Eurasian, and Pacific tectonic plates converge [1]. Indonesia is an area of intense volcanic and seismic activity due to the interactions between these tectonic plates [2,3]. The process of plate dynamics, which is quite intense, has also formed a distinct and quite varied relief of the earth's surface, ranging from mountainous regions with steep slopes that seem to imply a high potential for landslides to gently sloping coastal regions with potential threats of flooding, subsidence, and tsunamis [4,5]. It is preferable to be aware of the possible natural catastrophes that could occur so that we are able to mitigate their effects [6,7].

As the gateway to Papua and West Papua in particular, the city of Sorong is strategically located. The city of Sorong in the province of West Papua has significant potential as a national development hub and economic engine for the area. Hamid, the PUPR Ministry's Director General of Housing Provision, said that the first phase of development would target settlements, industrial regions, new city centres, and green open spaces between 2019 and 2028. As a sign of care for the road infrastructure in West Papua, the Deputy Minister of Indonesia's PUPR, Jhon Wempi Wetipo, planned road work during his visit to the Trans Sorong-Tambrauw road to inspect its condition. Wetipo, the Deputy Minister of Indonesia's PUPR, indicated that the 103-kilometre national road segment Sorong–Makbon-Mega is managed by the Sorong Region II Work Unit. The segment's functional length is 55.75 km, whereas the effective length of the dirt road is 33.5 km. This road segment also utilises the Multi Years Contract (MYC) plan for three budget years, 2020, 2021, and 2022, and is now in the bidding process due to one unsuccessful bidding procedure.

At the root of this issue, disorganised and imprecise land use planning is the primary cause of an increase in vulnerability [8]. To determine the possibility of each of these catastrophes, the method used must be based on their features and nature. Due to the fact that each kind of catastrophe has unique causes, a prospective analysis must be based on the factors that affect the disaster [9].

Similarities exist between mass movements and landslides [10,11]. To define an avalanche, it is important to describe both aspects. The movement of soil or rock masses in a vertical, horizontal, or oblique direction from their initial place is known as ground movement. Landslides and creep and flow movements comprise ground motion. According to this concept, avalanches are part of the ground's movement [12,13]. If, according to this definition, the vertical displacement of soil or rock masses is included in soil movement, then the vertical movement that occurs in bulging (deflection) owing to the collapse of the foundation may also be included in the kind of ground motion [14,15].

Material in the form of soil, or a combination of soil and rock fragments, will travel down the slope due to water infiltration into the pores of the rock or soil [16]. This state raises the stress on the slope surface material and represses the material and rock fragments, which might lead to the flow of material and water [17,18]. This results in road damage, the majority of which is caused by landslides in the corridor between Sorong and Makbon.

The degree of slope inclination has a direct correlation with sliding symptoms. As seen in the accompanying table, slope is often represented as one vertical slope and one horizontal slope. These physical measures make it simple to compile for slope stability analysis purposes. Table 1 shows the classification of slope categories that are on the underside of a pavement, along with suggested design considerations.

Slope degradation may be subdivided into mass movement and surface erosion, and slope is defined in angles by the ratio of the slope to the vertical.

On a sloped or non-horizontal surface, the force of gravity will make it easier for the soil mass to migrate downhill. The amount of gravitational force causes a reduction in shear resistance along the plane of the landslide, such that the soil's resistance is surpassed and a landslide occurs [19,20]. This investigation of the safety of a sloped ground surface is known as slope stability analysis. Typically, this approach is used for the construction of structures such as landfills, canals, dams, railways, airports, etc. [21]. The purpose of this study is to establish the safety of pavement side slopes, excavation slopes, and natural slopes. A slope fails owing to a reduction in soil stress or an increase in soil stress. Loads, stresses, geometries, and water conditions influence slopes. These may be permanent loads, such as their own weight, or transitory (dynamic from an explosion) [22,23].

From the literature that has been mentioned and reviewed in the previous description, it can be seen that the concern for earthquake loads is really specific only to structures that are categorised as "slope structures". Meanwhile, when talking about roads that are on slopes, there is very little in-depth analysis regarding the worst conditions that will occur, such as an earthquake. Most of the modelling carried out in Indonesia simply describes the earthquake load based on assumptions without looking at the history of earthquakes based on existing seismic data. As a result, in the vicinity of the area where this investigation was carried out, many road structures on slopes experienced failure, even when using massive structures such as concrete retaining walls combined with piles. Therefore, in this investigation, the authors try to provide an overview of the use of probabilistic seismic hazard analysis, which can be used to obtain a better approach to seismic conditions in cases where a road structure is on a slope that is in an earthquake-prone area. It is hoped that, with this investigation, the executors and those in charge of road management in Indonesia will be able to improve the quality of technical assessments so as to avoid repeated design-build processes that will only turn into construction waste and eat up the existing budget. Figure 1 below illustrates the definition of incline with a description of the comparison between the vertical (V) and horizontal (H) angles.

Table 1. Slope Measurement.

Description	Degree	Radian	Tangent	Percentages (%)	Vertical: Horizontal	Design Consideration
Flat	0	0.000	0.000	0	∞	Slope design with drainage
Medium	5	0.087	0.087	9	11.4	
	10	0.174	0.176	18	5.7	
Steep	11.3	0.197	0.200	20	5.0	
	15	0.262	0.268	27	3.7	
	18.4	0.322	0.333	33	3.00	
	20	0.349	0.364	36	2.75	
	25	0.436	0.466	47	2.14	
Very Steep	26.6	0.464	0.500	50	2.00	
	30	0.524	0.577	58	1.73	
	33.7	0.588	0.667	67	1.50	
	35	0.611	0.700	70	1.43	
	40	0.698	0.839	84	1.19	
Extremely	45	0.785	1.000	100	1.00	Reinforcement design with compacted soil slopes
Steeped Slope	50	0.873	1.192	119	0.84	
	55	0.960	1.428	143	0.70	
	60	1.047	1.732	173	0.58	
	63	1.107	2.000	200	0.50	
	65	1.134	2.145	214	0.47	
Subvertical	70	1.22	2.75	275	0.36	Reinforcement design with walls
	75	1.31	3.73	373	0.27	
	76	1.33	4.0	400	0.25	
	80	1.40	5.7	567	0.18	
	85	1.48	11.4	1143	0.09	
Vertical	90	1.57	∞	∞	0.00	

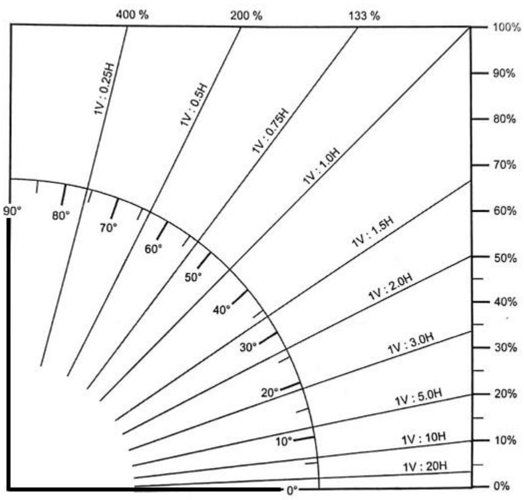

Figure 1. Inclination Definition (Source: [18]).

2. Methodology

The PSHA method is a probabilistic earthquake-hazard analysis method that takes into account and combines the uncertainty of the magnitude, location, and time of the earthquake's occurrence. The PSHA analysis is primarily a deterministic analysis with various scenarios and is not based only on the earthquake parameters that produce the greatest ground movement [24]. The main difference between the deterministic seismic hazard analysis (DSHA) and PSHA approaches is the probabilistic approach; the DSHA method does not consider the probability of an earthquake occurring and the influence of various uncertainties involved in the analysis, while the PSHA can predict the probability that the worst conditions will occur at a specific location, making it possible to account for the influence of uncertain factors such as size, location, and magnitude [25].

In constructing PSHA, earthquake source zones are classified into three types: (1) fault earthquake sources, or zones where earthquakes occur on faults with well-characterized mechanisms, slip rate, dip, fault length, and position. (2) The source of subduction earthquakes, especially the zone of occurrence of earthquakes around the point where oceanic and continental plates subduct under one another. The origin of subduction earthquakes is restricted to a depth of 50 km, or the megathrust zone. Quakes with a depth greater than 50 km will be identified as the cause of deep background quakes. (3) The source of the background earthquake (gridded seismicity), i.e., the source of the earthquake that is not yet fully understood but where several earthquakes have been detected [26]. The earthquake source model is divided into two distinct categories: shallow background (up to 50 km depth) and deep background (depth of more than 50 km). The deep background earthquake source model is separated into four depth intervals: 50–100 km, 100–150 km, 150–200 km, and 300 km [26]. The background earthquake source model uses a record of significant earthquakes that have been excluded by subduction and fault zone earthquakes [27].

In the PSHA approach, it is also important to analyse the attenuation function, which is a simple mathematical equation connecting the seismicity parameters at the epicentre (Magnitude, M, and Distance, R) with the ground motion parameters (acceleration spectra) at the review site. The attenuation function is a specific function created from earthquake data in a particular region, with time history serving as one of the variables required to construct the function. In addition to using the PSHA, it is important to compute the maximum ground acceleration value of the PGA in order to improve the accuracy of the seismic hazard analysis [28]. The computed PGA value is derived from the magnitude and the distance from the earthquake's epicentre. Analysis of seismic risk requires determination of the ground acceleration value, whereas the attenuation equation describes the link between ground vibration intensity, magnitude, and distance from the seismic source. Maximum ground vibration acceleration, or PGA, is one of the measures used to estimate seismic hazard conditions in a region. When it is essential to map the PGA using the PSHA approach in order to calculate the impacts of each seismic source, the PGA must be mapped using this method [29].

The results of this research are crucial for inputting parameters into simulations of slope stabilisation using finite element software such as PLAXIS and Geo Slope. Taking into account the findings of this investigation, it is anticipated that the modelling results utilising finite elements will tolerate severe situations such as earthquakes—particularly for the Sorong–Makbon route (Figure 2) itself (which is situated quite near to cliffs and hills as illustrated in Figure 3).

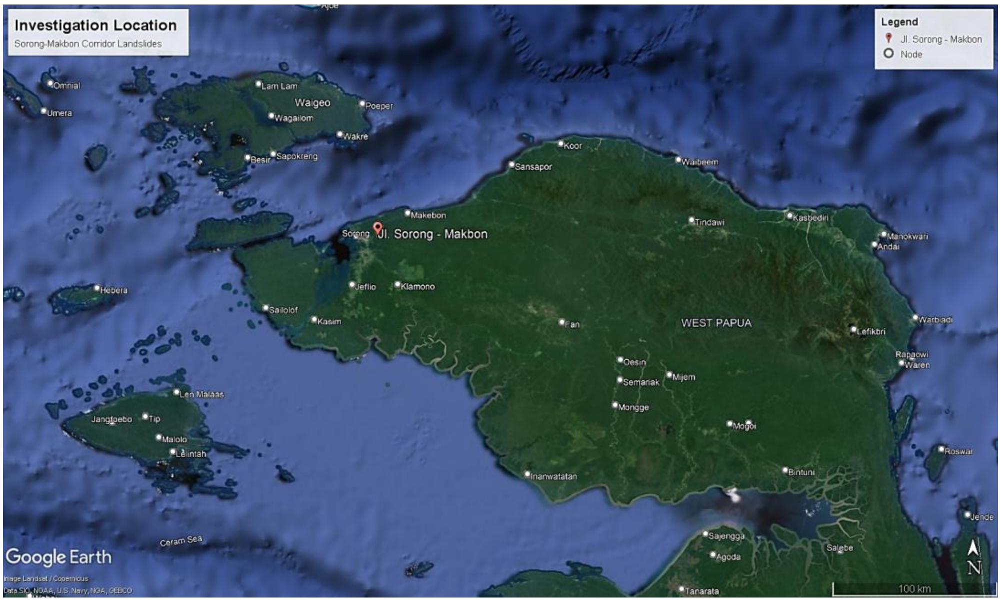

Figure 2. Investigation Location.

Figure 3. Typical Landslides.

3. Results and Discussion

Earthquake event data in the West Papua area for a period of 52 years, starting from 1970 to 2022, were obtained from the USGS catalogue with the boundaries of the review area and coordinate points, namely [−0.888744°]–[−0.842297°] Latitude and [131.346°] Longitude (where for the entire area of West Papua earthquake data were obtained for a total of 991 earthquake events with magnitudes ranging from 3 SR to 7.7 SR). Earthquake data were collected from this point using the incorporated research institutions for seismology (IRIS) catalogue. The coordinate points where the landslide was seen on the Sorong–Makbon road section are listed in the Table 2 and typical models of landslide that occur are shown in Figure 3.

From the IRIS catalogue data, data processing WAS then carried out through the application to analyse earthquakes probabilistically by PSHA. Figure 4 illustrates the visualization of earthquake distribution pattern data around the research area since 1970. Meanwhile, Figure 5 shows the maximum magnitude and slip rate of earthquake sources based on fault and plate paths from the perspective of the Indonesian archipelago. Before carrying out calculations using the PSHA method, it was necessary to first ascertain the types of earthquake sources. Earthquake sources are divided into 3 categories, namely:

1. The source of the earthquake fault is an upward fault or back arc that occurs on the mainland plate. Faults are also classified into two types: those caused by geometry and those caused by plate movement. In addition, the movement of the fault also consists of two directions of movement, namely dip and strike.
2. The source of subduction (subduction) earthquakes is a subduction zone or a location where two active tectonic plates collide. The release of energy due to the movement of these tectonic plates propagates in the form of waves, causing earthquakes somewhere. Subduction can be divided into two types based on the depth of the point of the earthquake, namely subduction interface (earthquake with a depth of 50 km) and subduction interslab (earthquake with a depth greater than 50 km).
3. The sources of background earthquakes are earthquake points whose sources have not been properly identified. Background earthquake sources are also classified based on their depth, with background interfaces (earthquakes with depth points of 50 km) and background interslab (earthquakes with depth points greater than 50 km) being the most common. The maximum depth limit of the source of this earthquake is 50 km, or the Megatrus area. The "deep background earthquake source model," which is Benioff earthquakes or earthquakes with a subduction zone with a steep dive angle, is used for deeper areas (50 km).

Table 2. Landslide Coordinates.

Num.	Corridor Registered Number	Corridor	KM/Station	Location Coordinate	
				Latitude	Longitude
1.	63.031	Sorong–Makbon	KM.15 + 250	0°53′19.48″ S −0.888744°	131°20′47.03″ E 131.346393°
2.	63.031	Sorong–Makbon	KM.16 + 900	0°52′52.81″ S −0.881336°	131°21′16.73″ E 131.354647°
3.	63.031	Sorong–Makbon	KM. 17 + 500	0°52′46.59″ S −0.879608°	131°21′31.63″ E 131.358786°
4.	63.031	Sorong–Makbon	KM. 19 + 450	0°51′59.02″ S −0.866394°	131°21′53.84″ E 131.364956°
5.	63.031	Sorong–Makbon	KM. 22 + 100	0°51′09.82″ S −0.852728°	131°22′44.90″ E 131.379139°
6.	63.031	Sorong–Makbon	KM. 23 + 300	0°50′42.19″ S −0.845053°	131°23′5.03″ E 131.384731°
7.	63.031	Sorong–Makbon	KM. 23 + 800	0°50′32.27″ S −0.842297°	131°23′6.07″ E 131.385019°

From the IRIS Catalogue data regarding the history of earthquakes that occurred in West Papua and its surroundings (Figure 4), several analyses were carried out in the application, namely:

1. Magnitude Scale Equalization, where the earthquake data that have been obtained in the form of the USGS catalogue is equalised to the magnitude scale because the earthquake source uses different earthquake scales such as local magnitude scale (mL), body magnitude (mb), surface magnitude (ms), and magnitude moment (M). In this case, the magnitude scale is converted to the moment magnitude scale (M) or $M \geq 4$, with the source and hypocentre distances of 200–500 km from the location or observation area of the earthquake source.
2. Separation of earthquakes (declustering) is the separation of earthquakes between the main earthquake (foreshock) and aftershocks (aftershocks) using the criteria of time span and distance.
3. Logic tree and determination of the attenuation function. This is done for the purpose of determining the weighting of each earthquake parameter in the use of seismic

hazard analysis and describing the level of confidence in the parameters used. This logic tree is also intended for weighting fault earthquake sources, subduction earthquake sources, and background earthquake sources by determining the attenuation function, where the attenuation function is a function of the ground movement acceleration data.

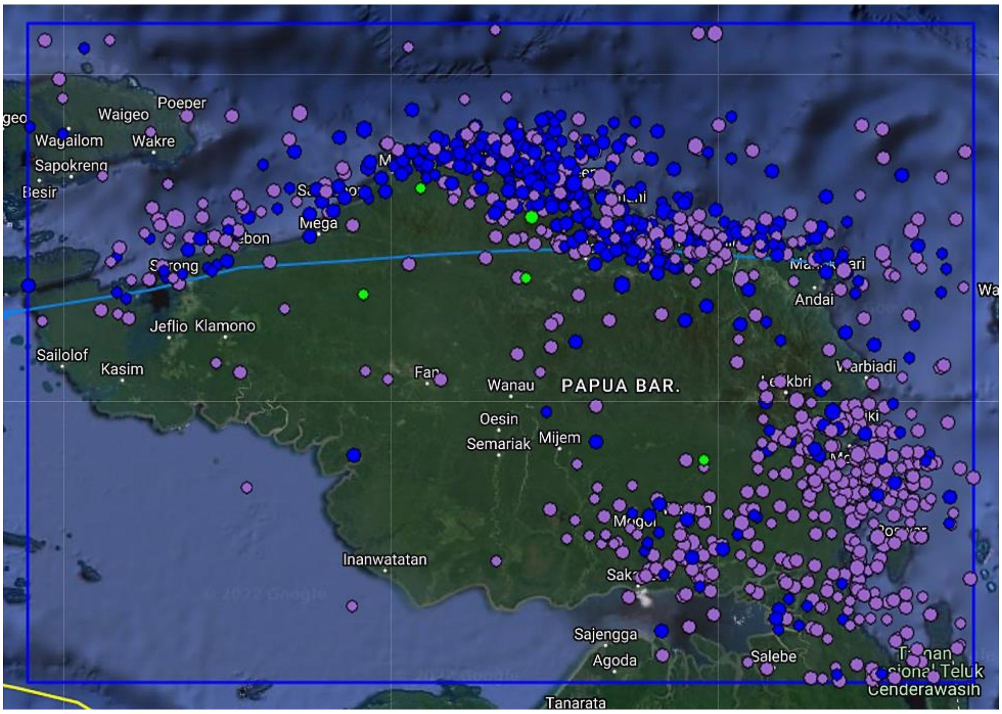

Figure 4. IRIS Catalogue for Historical Data on the Distribution Pattern of the West Papua Earthquake for the Period 1970–2022.

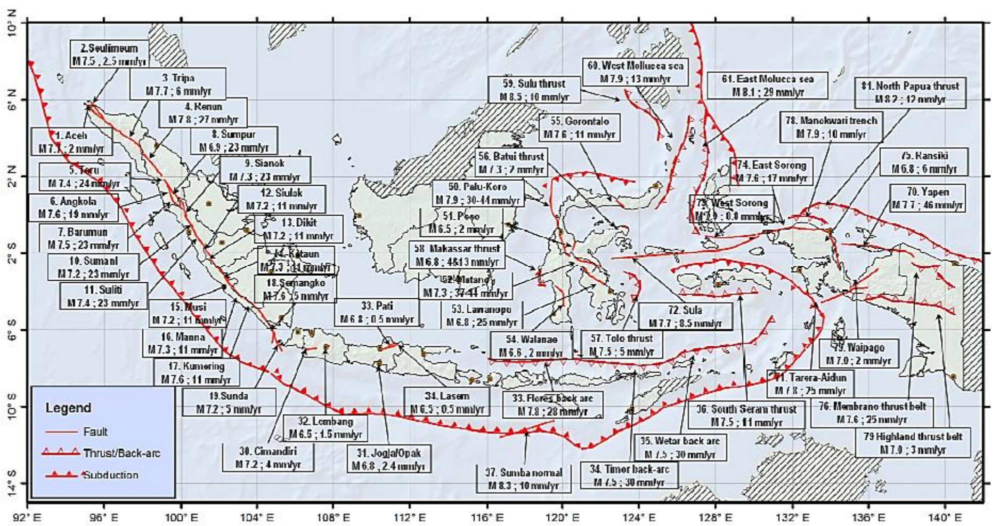

Figure 5. Maximum magnitude and slip-rate of earthquake sources.

IRIS Catalogue data from USGS sources for West Papua and its surroundings were then plotted in the software to facilitate PSHA analysis. Using Figures 4 and 5, the distribution of earthquakes around the study area can be interpreted and visualized based on the magnitude as shown in Figure 6 and then narrowed the scope specifically to the investigation area shown in Figure 7. The output can be seen in the figure below.

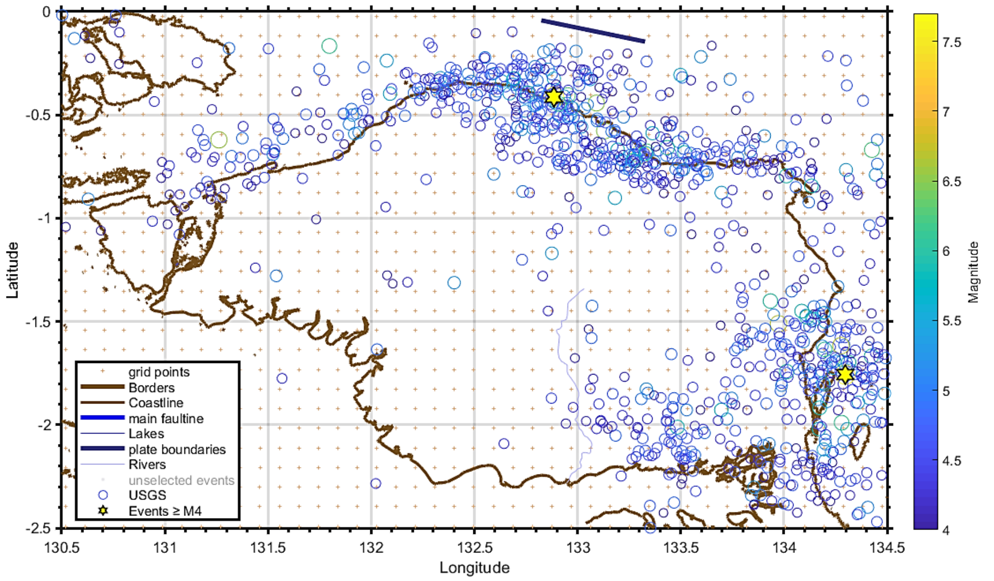

Figure 6. Distribution of West Papua earthquake events for the 1970–2022 period based on magnitude.

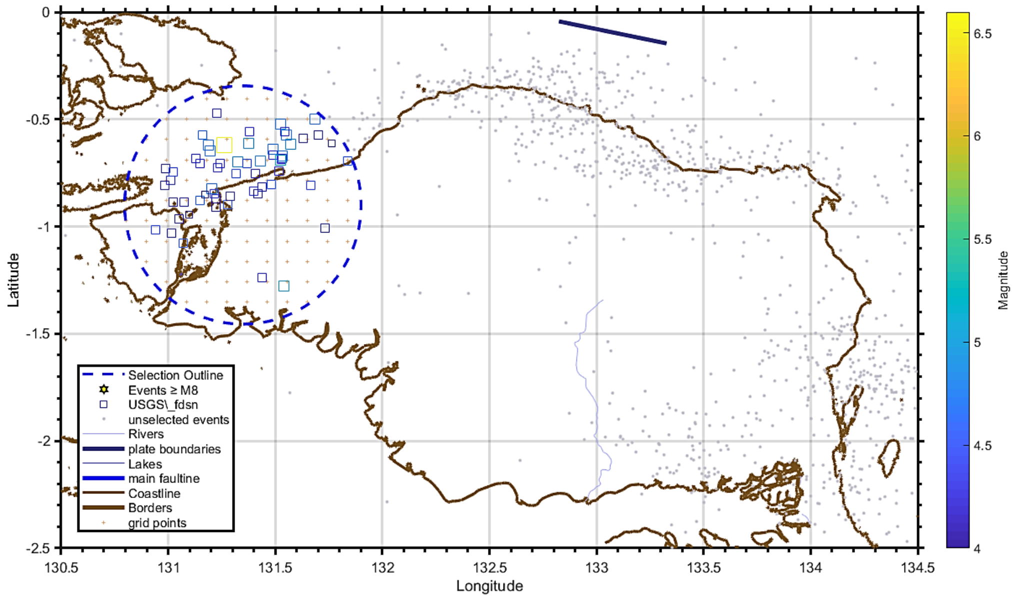

Figure 7. Distribution of Sorong-Makbon area earthquake events for the 1970-2022 period based on magnitude.

Data processing from the output of the software with uniformity of the magnitude scale and sorting of earthquake data according to the boundaries of the West Papua region with the review area, namely the Sorong–Makbon section and its surroundings, was carried out with the help of Microsoft Excel. The magnitude scale was then converted to one magnitude moment (M) $\geq$ 4 and the earthquake data of 59 earthquakes with magnitudes from 4 SR to 6.6 SR were obtained (Figures 5–7).

The converted data were then declustered with the help of the Matlab-Zmap software. Earthquake data around the Sorong-Makbon road section is then linked to the depth variable shown in Figure 8. Separation (declustering) aims to separate the main-shock earthquake, the aftershock, and the main earthquake. This separation will later become a reference for determining, characterizing, and modelling earthquake sources. The results of the separation (Declustering) obtained the remains of the earthquake with varying depths ranging from 10 km to a depth of 45 km (Figure 8).

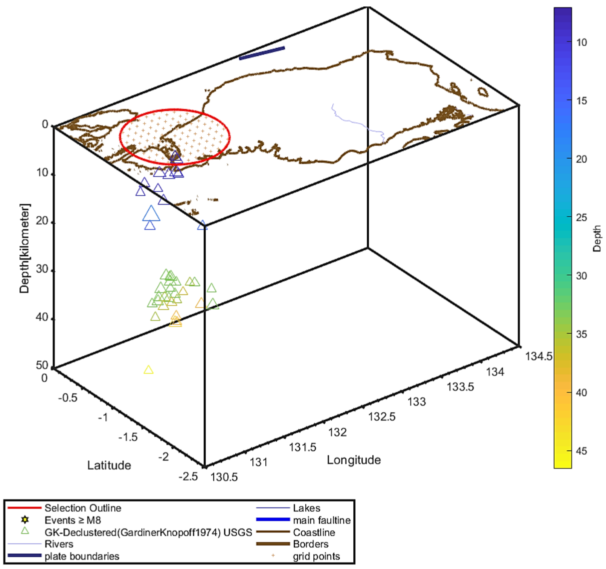

Figure 8. Declustering of earthquakes on the Sorong-Makbon section and its surroundings based on depth.

The modelling and characteristics of earthquake sources were carried out to analyse the impact of seismic hazards, which describe the historical occurrence of earthquakes in certain areas, in this case in the West Papua region, especially in the Sorong–MMakbon section. From this modelling, the parameters a and b were determined, which can be used to determine and predict the maximum value of the earthquake from the earthquake source. Parameters a and b were determined using software, which in this case uses the maximum likelihood method.

Tectonic parameters or b-values (b-values) can reflect local stress accumulation so that they can be seismic parameters obtained from the relative frequency of the number of large and small earthquakes in an area. The value of b is used to determine changes in the physical phenomena observed before the earthquake.

The seismic parameter, commonly called the a-value, is a seismic parameter whose value depends on the number of earthquake occurrences, volume, and time window that are within the limits of the review. The seismicity value can indicate the characteristics of the seismicity level data of an area, or in other words, describe the seismic activity in an area within a certain period of time, where the relationship between the distribution of earthquakes and depth, which is dominated by earthquakes with a depth of 100 km as shown in Figure 9.

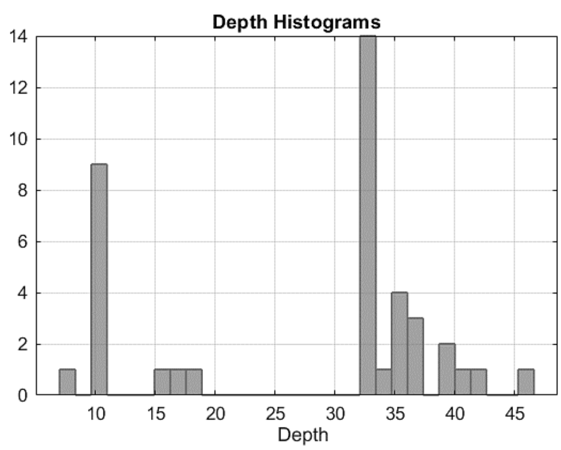

(**A**)

Figure 9. *Cont.*

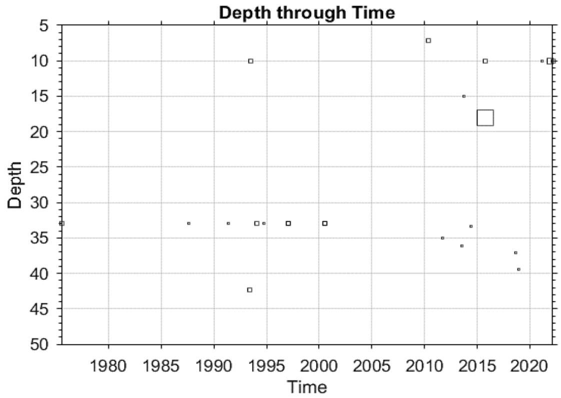

(**B**)

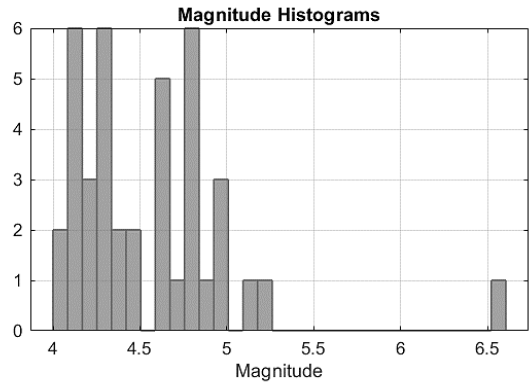

(**C**)

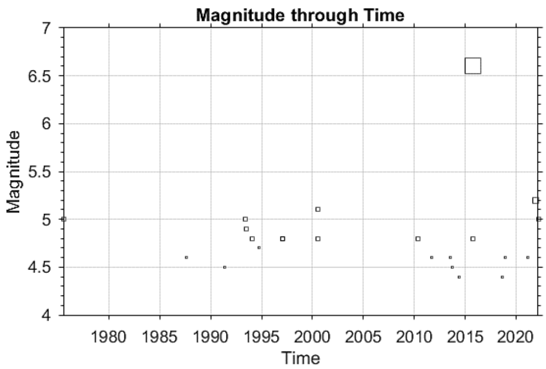

(**D**)

Figure 9. (**A**) Frequency Distribution with Depth; (**B**) Earthquake time period (Time) to Depth (Depth); (**C**) Frequency Distribution with Magnitude; (**D**) Earthquake time period (Time) against Magnitude on the Sorong-Makbon section.

While the graph of the relationship between magnitude and frequency shows a b-value of 0.980 for a standard value of 0.12 (Figure 9), this shows that the soil structure in the Sorong–Makbon section tends to be homogeneous, and with a b-value < 1, it indicates that this area has a high level of moderate seismicity. The relation between frequency of occurrence and magnitude is shown in Figure 10. The a-value is 5.780, and the magnitude of completeness (Mc) is 4.10(Figure 10). This a-value depends on the number of earthquake occurrences, volume, and time window that are within the limits of the review. The Mc value was based on the historical earthquake data of the catalogue for the Sorong–Makbon area since 1970. This means that from 1970 to the present, all earthquakes above a magnitude of 4.1 have been recorded in the catalogue from 1970 to the present time.

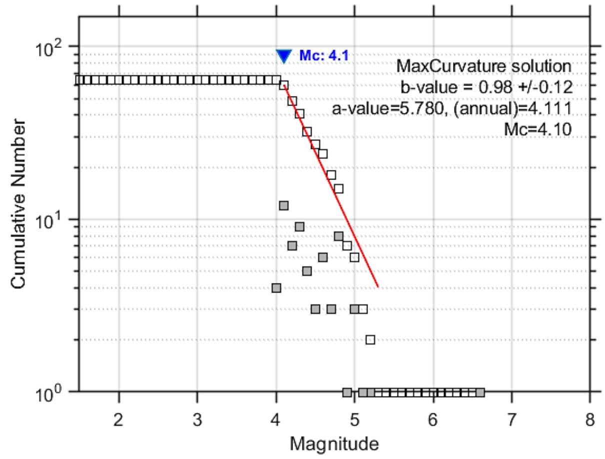

Figure 10. Relation between frequency of occurrence and magnitude.

From this case, a Response Spectrum calculation was carried out, where in the calculation of the Earthquake Acceleration refers to SNI 1726-2019 concerning Procedures for Planning Earthquake Resistance for Building Structures and Non-Buildings, SNI 8899-2020 concerning Procedures for Selection and Modification of Ground Surface Motion, and ISBN 978-602-5489-01-3 concerning the 2017 Indonesia Earthquake Source and Hazard Map issued by the National Center for Earthquake Studies of the Ministry of Public Works and Public Housing, where from this standard reference there are several provisions concerning parameters of earthquake acceleration. The value of the amplification factor for the frequency of earthquakes around the Sorong-Makbon road section is shown in Table 3. Whereas in Figure 11 the ground motion mapping is illustrated which is mapped based on color which describes the spectrum response of 1 s and 0.2 s respectively. Furthermore, the Recapitalization of Spectrum Response Values for Sorong–Makbon Section Points is shown in Table 4.

Table 3. The value of the Amplification Factor.

PGA and Period: 0.2 s (F_{pga} and F_a)					
Site Class	**PGA $\leq$ 0.1 $S_S \leq$ 0.25**	**PGA = 0.2 S_S = 0.5**	**PGA = 0.3 S_S = 0.75**	**PGA = 0.4 S_S = 1.0**	**PGA $\leq$ 0.5 $S_S \leq$ 1.25**
Hard Rock (SA)	0.8	0.8	0.8	0.8	0.8
Rock (SB)	1.0	1.0	1.0	1.0	1.0
Hard Soil (SC)	1.2	1.2	1.1	1.0	1.0
Medium Soil (SD)	1.6	1.4	1.2	1.1	1.0
Soft Soil (SE)	2.5	1.7	1.2	0.9	0.9
Special Soil (SF)	SS	SS	SS	SS	SS
Period: 1 s (Fv)					
Site Class	**$S_1 \leq$ 0.1**	**$S_1 \leq$ 0.2**	**$S_1 \leq$ 0.3**	**$S_1 \leq$ 0.4**	**$S_1 \leq$ 0.5**
Hard Rock (SA)	0.8	0.8	0.8	0.8	0.8
Rock (SB)	1.0	1.0	1.0	1.0	1.0
Hard Soil (SC)	1.7	1.6	1.5	1.4	1.3
Medium Soil (SD)	2.4	2.0	1.8	1.6	1.5
Soft Soil (SE)	3.5	3.2	2.8	2.4	2.4
Special Soil (SF)	SS *	SS	SS	SS	SS

SS *: Sites that require specific geotechnical investigations and site-specific response analysis refer to the determination of site classification based on SNI 1726:2019.

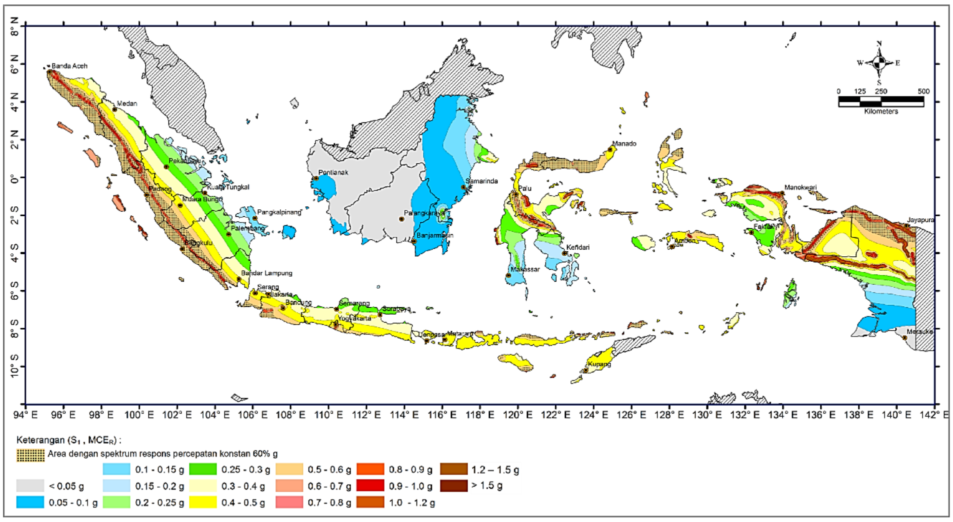

(**A**)

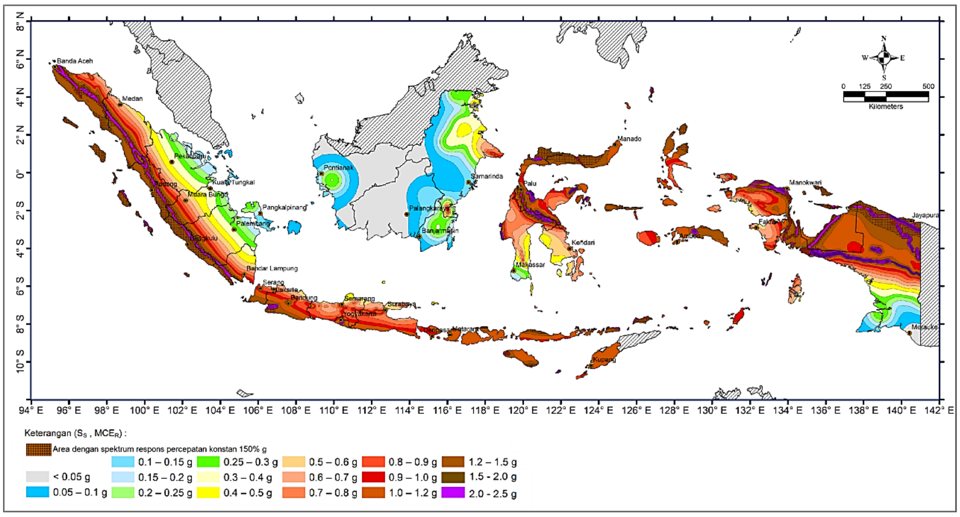

(**B**)

Figure 11. (**A**) Ground motion parameters, S1, maximum considered risk-targeted earthquake (MCER) for the Indonesian region 1 s response spectrum (critical attenuation 5%) at the BC site (SBC) (SNI 1726:2019); (**B**) Parameters of ground motion, Ss, maximum considered risk-targeted earthquake (MCER) for the Indonesian region response spectrum 0.2 s (critical attenuation 5%) at the BC site (SBC) (SNI 1726:2019).

Next, the site coefficients of Fa and FV were determined based on SS and S1 values. To determine Ss and S1 values, data generated from the Spektra Response Program software, Puskim-Pusgen 2019, and Earthquake Map are used.

It is quite difficult to find a comparison for this investigation because all of the modelling of roads on slopes using the finite element method, such as the PLAXIS program, do not take into account earthquake loads using the PSHA method. Thus, comparisons can only be made after there are results of analysis from the same process, in this case modelling using a finite element device, when it will be possible to see the differences in the output characteristics produced. This is because, in assuming earthquake loads, most models only add a multiplier factor to the loads that occur uniformly—unlike the case with the PHSA method which can provide more specific results based on historical data of earthquakes that have occurred in a location. Of course, the most striking difference between the two is the design criteria. If you only use the multiplier factor, you can judge that the assumption will be immature and can actually cause structural instability when an earthquake occurs because the earthquake load is assumed to be an additional load.

By contrast, the PHSA method is able to provide a more thorough and structured picture, even for several different points. Of course, this is influenced by the distance of different points from the earthquake location. The effect is that over-design can occur in a structure, which is why the results of the analysis on the finite element will give a large safety factor value because the earthquake load is considered an additional load with a multiplier factor that will be applied uniformly at all test points. However, looking at the events in the field where this investigation was carried out shows otherwise.

Table 4. Recapitulation of Spectrum Response Values for Sorong–Makbon Section Points.

Item	Unit	Value						
Sta.	-	15 + 250	16 + 900	17 + 500	19 + 450	22 + 100	23 + 300	23 + 800
Longitude	(*)	131.34639	131.35465	131.35879	131.36496	131.37914	131,384,731	131,385,019
Latitude	(°)	−0.888744	−0.881336	−0.879608	−0.866394	−0.852728	−0.845053	−0.842297
Site Class	-	SD	SD	SC	SC	SD	SD	SD
PGA	gal	0.4946	0.49876	0.49876	0.511031	0.521365	0.528557	0.531793
PGAm	gal	0.54673	0.54926	0.59852	0.613237	0.573501	0.581413	0.584972
CRs	-	0	0	0	0	0	0	0
CR1	-	0	0	0	0	0	0	0
Ss	gal	126,491	127,413	127,382	1.305013	1.333556	1,353,878	1,362,628
S1	gal	0.51201	0.51499	0.51465	0.526156	0.536494	0.5441	0.547441
TL	sec	11,000	11,000	11,000	10,000	10,000	9000	9000
Fa	-	1000	1000	1200	1200	1000	1000	1000
Fv	-	178,800	178,501	148,535	1,473,844	1,763,506	17,559	1.752559
Sms	gal	1.26491	1.27413	152,858	1,566,015	1,333,556	1,353,878	1,362,628
Sm1	gal	0.91546	0.91926	0.76444	0.775472	0.946111	0.955386	0.959422
Sds	gal	0.84327	0.84942	101,906	104,401	0.889037	0.902585	0.908419
Sd1	gal	0.61031	0.61284	0.50963	0.516981	0.63074	0.636924	0.639615
TO	sec	0.14475	0.1443	0.10002	0.099038	0.141893	0.141133	0.140819
Ts	sec	0.72374	0.72148	0.5001	0.495188	0.709465	0.705666	0.704097

4. Conclusions

Based on the results of the analysis that has been described, an acceleration value (PGA) of between 1.2 and 1.5 G was obtained. This confirms the cause of the large number of landslides on the Sorong–Makbon section, considering that the area and the surrounding areas are prone to the effects of earthquakes. In view of this, it is recommended that the design of the handling and strengthening of roads and slopes in the Sorong–Makbon Section use a retaining wall with a combination of bore piles to increase slope stability.

Based on the investigations in this study, the mapping of earthquake areas and their effects has a major impact on the design of a structure. As a fundamental design concept in engineering, factors like this must be taken into account and become one of the worst condition assumptions that could occur. Thus, the resulting design will certainly have a greater safety factor. When compared with the cost, of course, further reviews will be needed.

This investigation found that most modelling using the finite element method, like the PLAXIS programme, does not adequately take earthquake loads into account when modelling roads on slopes. The inclusion of the PHSA method can give more specific results based on historical data of earthquakes that have happened in a location. The most important difference between the two is how they were made, as most models only add a multiplier factor to the loads that happen uniformly. The result is that a structure can be over-designed, which is why the finite element analysis will give a high safety factor. However, what happened in the field where this investigation was done shows that this is not true.

Funding: This research received no external funding.

Institutional Review Board Statement: Not applicable.

Data Availability Statement: Not applicable.

Acknowledgments: The author acknowledges Pusat Studi Perencanaan Pembangunan Pengembangan Prasarana (PSP4) for all the support along the investigation.

Conflicts of Interest: The author declares no conflict of interest.

References

1. Ansari, A.; Rao, K.; Jain, A.K. Seismic Hazard and Risk Assessment in Maharashtra: A Critical Review. *Lect. Notes Civ. Eng.* **2021**, *116*, 35–45. [CrossRef]
2. Aristizábal, C.; Bard, P.Y.; Beauval, C.; Gómez, J.C. Integration of site effects into probabilistic seismic hazard assessment (PSHA): A comparison between two fully probabilistic methods on the euroseistest site. *Geosciences* **2018**, *8*, 285. [CrossRef]
3. Caroles, L. Hubungan Nilai Modulus Kekakuan Pada Alat Marshall Test Terhadap Alat Light Weight Deflectometer (Lwd) Laboratorium. 2021. Available online: http://repository.unhas.ac.id/id/eprint/4160/ (accessed on 26 January 2023).
4. Caroles, L. *Pengantar Perkerasan dan Landasan*, 1st ed.; Wawasan Ilmu: Kuala Klawang, Malaysia, 2022; Available online: https://www.google.com/books?hl=en&lr=&id=rA-mEAAAQBAJ&oi=fnd&pg=PA1&dq=Lucky+caroles&ots=zbtmr8eEjl&sig=bBttDqei5FdibYDsnXC_vR4rs7E (accessed on 26 January 2023).
5. Caroles, L. *Pengantar Preservasi Dan Survey Kondisi Jalan*; Wawasan Ilmu: Kuala Klawang, Malaysia, 2022; Available online: https://www.google.com/books?hl=en&lr=&id=932nEAAAQBAJ&oi=fnd&pg=PA37&dq=Lucky+caroles&ots=GMV7UpFi5C&sig=5cA0MIknR2gfQjrWT7-WaDISY3M (accessed on 26 January 2023).
6. Chioccarelli, E.; Cito, P.; Iervolino, I.; Giorgio, M. REASSESS V2.0: Software for single- and multi-site probabilistic seismic hazard analysis. *Bull. Earthq. Eng.* **2019**, *17*, 1769–1793. [CrossRef]
7. Ebrahimian, H.; Jalayer, F.; Forte, G.; Convertito, V.; Licata, V.; d'Onofrio, A.; Santo, A.; Silvestri, F.; Manfredi, G. Site-specific probabilistic seismic hazard analysis for the western area of Naples, Italy. *Bull. Earthq. Eng.* **2019**, *17*, 4743–4796. [CrossRef]
8. Gerstenberger, M.C.; Marzocchi, W.; Allen, T.; Pagani, M.; Adams, J.; Danciu, L.; Field, E.H.; Fujiwara, H.; Luco, N.; Ma, K.F.; et al. Probabilistic Seismic Hazard Analysis at Regional and National Scales: State of the Art and Future Challenges. *Rev. Geophys.* **2020**, *58*. [CrossRef]
9. Griffin, J.; Nguyen, N.; Cummins, P.; Cipta, A. Historical earthquakes of the eastern sunda arc: Source mechanisms and intensity-based testing of Indonesia's national seismic hazard assessment. *Bull. Seismol. Soc. Am.* **2019**, *109*, 43–65. [CrossRef]
10. Hendriyawan, H.; Aditramulyadi, D.D.; Syahbana, A.J. Seismic hazard analyses for North Java Offshore Indonesia using ISO 19901-2:2004. *IOP Conf. Ser. Earth Environ. Sci.* **2021**, *729*, 012006. [CrossRef]
11. Irsyam, M.; Cummins, P.R.; Asrurifak, M.; Faizal, L.; Natawidjaja, D.H.; Widiyantoro, S.; Meilano, I.; Triyoso, W.; Rudiyanto, A.; Hidayati, S.; et al. Development of the 2017 national seismic hazard maps of Indonesia. *Earthq. Spectra* **2020**, *36*, 112–136. [CrossRef]
12. Jena, R.; Pradhan, B.; Beydoun, G.; Nizamuddin; Ardiansyah; Sofyan, H.; Affan, M. Integrated model for earthquake risk assessment using neural network and analytic hierarchy process: Aceh province, Indonesia. *Geosci. Front.* **2020**, *11*, 613–634. [CrossRef]
13. Lewerissa, R.; Rumakey, R.; Syakur, Y.A.; Lapono, L. Completeness magnitude (Mc) and b-value characteristics as important parameters for future seismic hazard assessment in the West Papua province Indonesia. *Arab. J. Geosci.* **2021**, *14*, 2588. [CrossRef]
14. Makrup, L.; Sodik, H.M.; Winarno, S.; Suryo, B.; Sunardi, B. Soil surface seismic hazard maps for yogyakarta, indonesia based on probabilistic seismic hazard analysis, code and global VS30. *Int. J. Civ. Eng. Technol.* **2018**, *9*, 637–648. Available online: https://www.academia.edu/download/58382056/SOIL_SURFACE_SEISMIC_HAZARD_MAPS_FOR_YOGYAKARTA.pdf (accessed on 26 January 2023).
15. Nas, M.; Lyubushin, A.; Softa, M.; Bayrak, Y. Comparative PGA-driven probabilistic seismic hazard assessment (PSHA) of Turkey with a Bayesian perspective. *J. Seismol.* **2020**, *24*, 1109–1129. [CrossRef]
16. Ordaz, M.; Salgado-Gálvez, M.A.; Giraldo, S. R-CRISIS: 35 years of continuous developments and improvements for probabilistic seismic hazard analysis. *Bull. Earthq. Eng.* **2021**, *19*, 2797–2816. [CrossRef]
17. Papadopoulos, A.N.; Bazzurro, P.; Marzocchi, W. Exploring probabilistic seismic risk assessment accounting for seismicity clustering and damage accumulation: Part I. Hazard analysis. *Earthq. Spectra* **2021**, *37*, 803–826. [CrossRef]
18. Paulus, K.; Basuki, H. *Applied Geotechnics for Engineers*, 2nd ed.; Giovanny, R., Ed.; ANDI: Yogyakarta, Indonesia, 2020.
19. Pei, W.; Zhou, S.; Zhuang, J.; Xiong, Z.; Piao, J. Application and discussion of statistical seismology in probabilistic seismic hazard assessment studies. *Sci. China Earth Sci.* **2022**, *65*, 257–268. [CrossRef]
20. Pothon, A.; Gueguen, P.; Buisine, S.; Bard, P.Y. Comparing Probabilistic Seismic Hazard Maps with ShakeMap Footprints for Indonesia. *Seismol. Res. Lett.* **2020**, *91*, 847–858. [CrossRef]
21. Puteri, D.M.; Affandi, A.K.; Sailah, S.; Hudayat, N.; Zawawi, M.K. Analysis of peak ground acceleration (PGA) using the probabilistic seismic hazard analysis (PSHA) method for Bengkulu earthquake of 1900–2017 period. *J. Phys. Conf. Ser.* **2019**, *1282*, 012054. [CrossRef]
22. Rahman, A.U.; Najam, F.A.; Zaman, S.; Rasheed, A.; Rana, I.A. An updated probabilistic seismic hazard assessment (PSHA) for Pakistan. *Bull. Earthq. Eng.* **2021**, *19*, 1625–1662. [CrossRef]

23. Rahman, M.Z.; Siddiqua, S.; Kamal, A.S.M.M. Seismic source modeling and probabilistic seismic hazard analysis for Bangladesh. *Nat. Hazards* **2020**, *103*, 2489–2532. [CrossRef]
24. Sianko, I.; Ozdemir, Z.; Khoshkholghi, S.; Garcia, R.; Hajirasouliha, I.; Yazgan, U.; Pilakoutas, K. A practical probabilistic earthquake hazard analysis tool: Case study Marmara region. *Bull. Earthq. Eng.* **2020**, *18*, 2523–2555. [CrossRef]
25. Stevens, V.L.; Shrestha, S.N.; Maharjan, D.K. Probabilistic seismic hazard assessment of Nepal. *Bull. Seismol. Soc. Am.* **2018**, *108*, 3488–3510. [CrossRef]
26. Tromans, I.J.; Aldama-Bustos, G.; Douglas, J.; Lessi-Cheimariou, A.; Hunt, S.; Daví, M.; Musson, R.M.W.; Garrard, G.; Strasser, F.O.; Robertson, C. Probabilistic seismic hazard assessment for a new-build nuclear power plant site in the UK. *Bull. Earthq. Eng.* **2019**, *17*, 1–36. [CrossRef]
27. Villani, M.; Lubkowski, Z.; Free, M.; Musson, R.M.W.; Polidoro, B.; McCully, R.; Koskosidi, A.; Oakman, C.; Courtney, T.; Walsh, M. A probabilistic seismic hazard assessment for Wylfa Newydd, a new nuclear site in the United Kingdom. *Bull. Earthq. Eng.* **2020**, *18*, 4061–4089. [CrossRef]
28. Walker, J.P.F.; Visini, F.; Roberts, G.; Galasso, C.; McCaffrey, K.; Mildon, Z. Variable fault geometry suggests detailed fault-slip-rate profiles and geometries are needed for fault-based probabilistic seismic hazard assessment (PSHA). *Bull. Seismol. Soc. Am.* **2019**, *109*, 110–123. [CrossRef]
29. Wang, S.; Werner, M.J.; Yu, R. How Well Does Poissonian Probabilistic Seismic Hazard Assessment (PSHA) Approximate the Simulated Hazard of Epidemic-Type Earthquake Sequences? *Bull. Seismol. Soc. Am.* **2022**, *112*, 508–526. [CrossRef]